

Fluctuating wind loads on roof cladding fasteners and batten-truss connections

J. D. Ginger

Cyclone Structural Testing Station (CSTS), School of Engineering
James Cook University, Townsville, AUSTRALIA

Introduction

Studies have shown that regions under the separated shear layer, at the edges of a roof experience large suction pressures [1, 2]. Large positive internal pressures created by a breach in the windward wall combined with these external suction pressures result in large net uplift pressures and is mainly responsible for roof cladding failure during windstorms.

Thin-gauge steel (~0.6mm), “top-hat” battens are increasingly replacing the traditional 40 mm deep timber battens in low-rise house roof construction. These battens are typically placed at ~ 1.0 m intervals and screwed to roof trusses installed up to 1.2 m apart. The roof cladding is attached to the battens by fasteners at a spacing of 150 to 200 mm. Each cladding fastener takes wind loads acting on an area of about 0.2 m², whereas the batten-truss connection bears wind loads acting on a roof tributary area 1.0 m × 1.2 m, which is six times the area supported by a cladding fastener. As in the case of cladding fasteners, batten-truss connections near the ridge and eaves can experience large loads and are susceptible to fatigue failure at loads smaller than the “static” design load. This is a cause for concern as significant damage to large parts of a roof could arise from such fatigue failure.

The performance of roof systems designed for cyclone prone regions of Australia are evaluated according to TR 440 [3] and AS1170.2 [4], by applying cyclic loads in the following sequence: 8000 cycles at 0-0.40 p_d, 2000 cycles at 0-0.50 p_d, 200 cycles at 0-0.65 p_d and 1 cycle at 0-1.0 p_d, where p_d is the ultimate limit state net design pressure. AS1170.2 prescribes a local pressure factor K₁ of 1.5 and 2.0 to be applied with negative pressures on areas of extent less than 1.0a² and 0.25a² within a distance of 1.0a and 0.5a respectively from roof edges, where ‘a’ is taken to be the minimum of 0.2 × breadth(b) or 0.2 × depth(d) or height(h) of the structure. The validity applying such pressure factors on an area such as a batten-truss connection tributary is investigated in this study. The pressure characteristics on panels representative of cladding fastener and batten-truss connection tributaries, obtained from the full-scale Texas Tech building and a wind tunnel study on a typical low-rise house roofs are studied in this paper.

Theory

The pressure fluctuations on the roof (described by the pressure coefficient C_p, referenced to the mean dynamic pressure at the roof height) are analysed to give the mean value over time C_{p̄}, the standard deviation C_{σp}, maximum C_{p̄}, and minimum C_{p̄}. A normalised pressure g_p = (C_p - C_{p̄})/C_{σp} is defined such that maximum and minimum, pressure peak factors are g_{p̄} = (C_{p̄} - C_{p̄})/C_{σp} and g_{p̄} = (C_{p̄} - C_{p̄})/C_{σp}. Many model and full-scale studies [2, 5] have shown that the probability density function pf(g_p) of pressure fluctuations in separated flow regions is not of the Gaussian form of Eqn 1, but negatively skewed. The pressure spectra under the separated flow regions showed that energy is distributed towards higher frequencies compared to the approach velocity and windward wall pressure fluctuations [1].

$$p_f(g_p) = (1/\sqrt{2\pi}) \exp^{-\left(g_p^2/2\right)} \quad (1)$$

Experimental Set Up

Ginger et al [6] described the CSTS wind tunnel study carried out at 1/50 in terrain category 3 AS1170.2, on a $7.5 \times 15.6 \times 2.5$ m house with roof pitch of 20° , shown in Fig. 1. Each tributary area supported by trusses A, B, C..N spaced 1.2m apart was divided into panels 1..12 representing areas being supported by batten truss connections. Results showed that the areas near the windward gable end and ridge experienced large suction pressures. Based on the study by Ginger et al [6], wind pressure characteristics on flow separation areas near the eaves, ridge and gable end, and the inner part of the roof for a range of approach wind directions, θ were selected for further study. Each panel area on the roof is identified by the truss and panel numbers, such that B06 refers to panel 6 on truss B etc. The pressure characteristics on $1.0 \text{ m} \times 0.2 \text{ m}$ and $1.0 \text{ m} \times 1.8 \text{ m}$ areas defined as A and B, representative of a cladding fastener and a batten truss tributaries respectively at the windward leading edge of the full-scale Texas Tech building roof shown in Fig. 2, for $\theta = 90^\circ$ were also studied.

Results and Conclusions

Tables 1 and 2 give the C_{ps} and g_{ps} obtained from the Texas Tech full-scale study and the CSTS model study and peak C_{ps} derived from AS1170 (including K_1 factors). Internal, external and net C_p vs time plots for $\theta = 90^\circ$ on areas A and B of the Texas Tech building with a 2% windward wall opening are shown in Figs. 3 and 4. The probability distributions of the pressure fluctuations on A and B are compared with the Gaussian form in Figs. 5 and 6. Figs 7 and 8 show the probability distributions of external pressure fluctuations on edge and inner areas of the CSTS model building roof for $\theta = 30^\circ$ and 90° respectively.

Table 1 shows that large external and net suction $C_{\bar{p}}$ s were measured on areas A and B in the full-scale study. The net suction $C_{\bar{p}}$ on area A, exceeded values derived from AS1170.2 but compared favourably on area B. External and net $g_{\bar{p}}$ s on A and B were < -5 indicating the negative skewness in $pf(g_p)$ seen in Figs. 5 and 6. The CSTS model test results in Table 2, show that large external suction $C_{\bar{p}}$ s were measured on panel areas near the ridge and windward gable end, where $g_{\bar{p}}$ s were < -6 and $pf(g_p)$ s were negatively skewed. Wind tunnel tests generally underestimate peak suction pressures, and hence the degree of conservativeness of the AS1170.2 values is misleading. In the inner roof regions, $g_{\bar{p}}$ s were ~ 4 and $pf(g_p)$ s were closer to Gaussian. Although pressures on a fastener (area 0.2 m^2) can be underestimated, AS1170.2 provides satisfactory net design C_{ps} on tributary areas of 1.5 to 2.0 m^2 near roof edges. Roof areas of $0.07a^2$ and $0.7a^2$ within a distance $0.5a$ and $1.0a$ respectively from the edge experience pressures of similar characteristics.

References:

1. J. D. Ginger and C. W. Letchford, (1997) "Net pressures on a low-rise full scale building", Proc. 4APSOWE, Gold Coast Australia.
2. J. D. Ginger and C. W. Letchford, (1993) "Characteristics of large pressures in regions of flow separation", JWEIA, Vol. 49, 301-310.
3. Technical Record 440 (TR 440), (1983) "Guidelines for the testing and evaluation of products for cyclone-prone areas.
4. Australian Standard SAA Loading Code Part 2 Wind Loads AS1170.2 (1989)
5. Y. L. Xu, (1993) "Wind Induced Fatigue Loading on Roof Cladding of Low-Rise Buildings", James Cook Uni. CSTS Technical Report No. 41
6. J. D. Ginger, G. F. Reardon and B. J. Whitbread, (1998) "Wind Loads on Roof Trusses", Proc. Australasian Structural Engineering Conference, New Zealand.

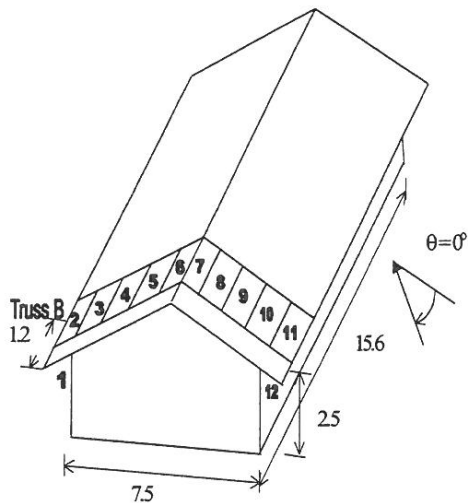


Fig. 1 7.5 × 15.6 × 2.5 m 20° roof pitch low-set building tested at 1/50 in the CSTS wind tunnel.

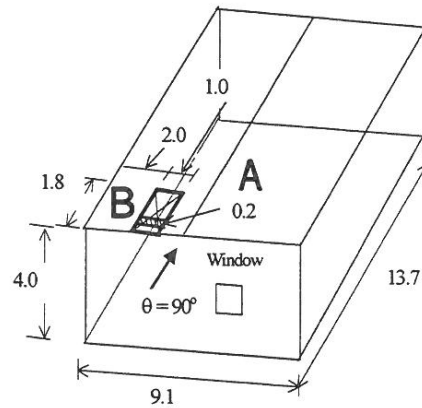


Fig. 2 13.7 × 9.1 × 4.0 m Texas Tech full-scale building showing windward roof edge regions A (1.0 × 0.2 m²) and B (1.0 × 1.8 m²)

Table 1 Pressure coefficients and pressure peak factors on Texas Tech full-scale building

Tribut	Area, m ²	$C_{\bar{p}}$	$C_{\bar{p}}$	$C_{\bar{p}}$	C_{σ_p}	$g_{\bar{p}}$	$g_{\bar{p}}$	$C_{\bar{p},\bar{p}}$ AS1170
$\theta = 90^\circ$								$\theta = 90^\circ$
Internal		0.65	2.80	-0.24	0.40	5.37	-2.23	2.14
A	0.2 (0.06a ²)	-1.43	-0.28	-7.10	0.60	1.93	-9.52	-5.51
B	1.8 (0.54a ²)	-1.37	-0.31	-4.50	0.54	1.99	-5.81	-4.82
A Net	0.2 (0.06a ²)	-2.08	-0.34	-8.36	0.88	1.97	-7.14	-7.65
B Net	1.8 (0.54a ²)	-2.02	-0.35	-6.36	0.84	1.97	-5.14	-6.96

Table 2 External pressure coefficients and pressure peak factors on CSTS model house

Tribut	Area, m ²	$C_{\bar{p}}$	$C_{\bar{p}}$	$C_{\bar{p}}$	C_{σ_p}	$g_{\bar{p}}$	$g_{\bar{p}}$	$C_{\bar{p},\bar{p}}$ AS1170
$\theta = 30^\circ$								$\theta = 0^\circ$
A04	0.79 (0.35a ²)	-1.28	-0.20	-3.49	0.42	2.54	-5.23	-4.46
A06	0.36 (0.16a ²)	-1.68	-0.31	-4.79	0.57	2.43	-5.49	-4.8
B04	1.57 (0.70a ²)	-0.77	-0.06	-2.44	0.29	2.45	-5.77	-3.46
B06	0.71 (0.32a ²)	-1.44	-0.30	-4.27	0.50	2.27	-5.65	-4.70
D06	0.71 (0.32a ²)	-1.03	-0.22	-2.89	0.33	2.38	-5.63	-4.56
G09	1.57 (0.70a ²)	0.08	0.89	-0.55	0.15	5.24	-4.10	-1.32, 0.56
$\theta = 90^\circ$								$\theta = 90^\circ$
A04	0.79 (0.35a ²)	-0.76	0.32	-3.27	0.36	3.04	-7.03	-6.70
A06	0.36 (0.16a ²)	-0.76	0.27	-3.45	0.39	2.64	-6.92	-7.2
B04	1.57 (0.70a ²)	-0.63	0.42	-2.52	0.31	3.35	-6.07	-5.18
B06	0.71 (0.32a ²)	-0.60	0.44	-2.78	0.33	3.21	-6.72	-7.06
D06	0.71 (0.32a ²)	-0.12	0.77	-1.59	0.20	4.35	-7.19	-3.80
G04	1.57 (0.70a ²)	0.03	0.52	-0.48	0.09	5.16	-5.47	-1.0

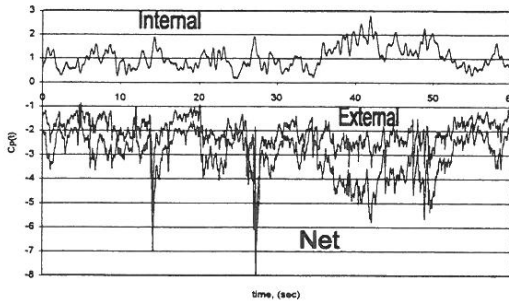


Fig 3. Part of internal and external and net Cp vs time on area A Texas Tech building.

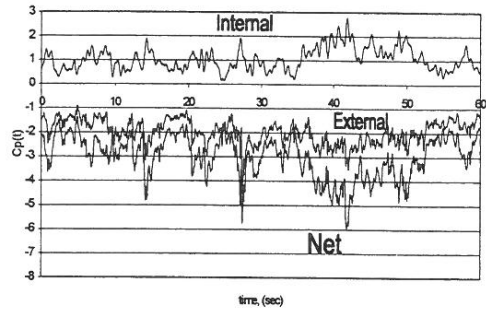


Fig 4. Part of internal and external and net Cp vs time on area B Texas Tech building.

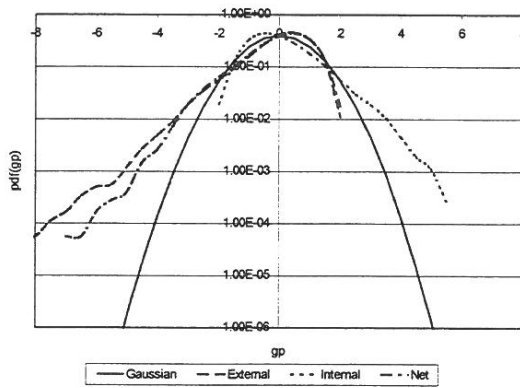


Fig 5 Probability density function of internal, external and net pressures on area A Texas Tech building

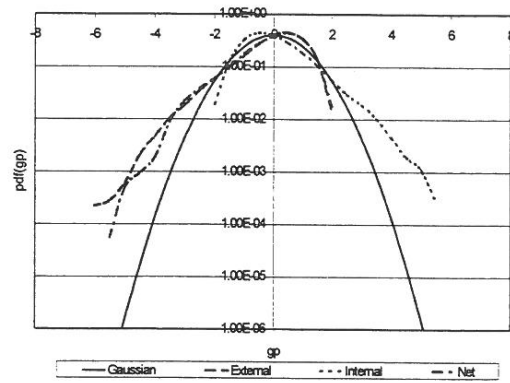


Fig 6 Probability density function of internal, external and net pressures on area B Texas Tech building

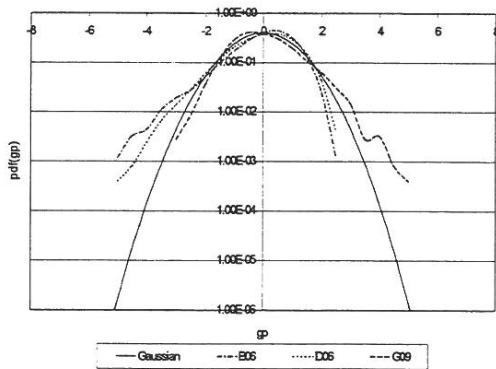


Fig 7 Probability density function of external pressures on parts of CSTS model building for $\theta = 30^\circ$

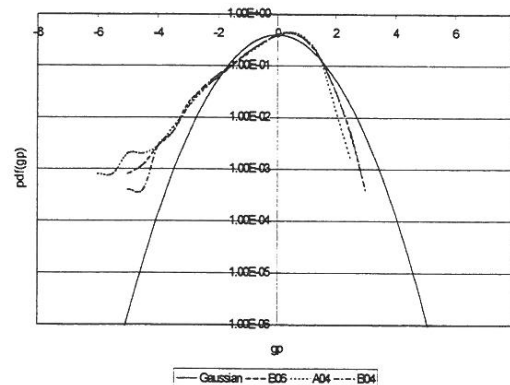


Fig 8 Probability density function of external pressures on parts of CSTS model building for $\theta = 90^\circ$